ACS Sustainable Chemistry & Engineering

Research Article

pubs.acs.org/journal/ascecg

Effective Upgrade of Levulinic Acid into γ-Valerolactone over an Inexpensive and Magnetic Catalyst Derived from Hydrotalcite Precursor

Jun Zhang,[†] Jinzhu Chen,*[,†] Yuanyuan Guo,[†] and Limin Chen[‡]

[†]CAS Key Laboratory of Renewable Energy, Guangzhou Institute of Energy Conversion, Chinese Academy of Sciences, Guangzhou 510640, P.R. China

[‡]School of Environment and Energy, South China University of Technology, Guangzhou Higher Education Mega Centre, Guangzhou 510006, P.R. China

Supporting Information

ABSTRACT: A low-cost and magnetic catalyst derived from a hydrotalcite precursor was developed for selective hydrogenation of levulinic acid (LA) into γ-valerolactone (GVL) in a methanol solvent. An excellent GVL yield of 98.1% with full LA conversion was achieved at 415 K over a magnetic and recyclable $Ni_{4.59}Cu_1Mg_{1.58}Al_{1.96}Fe_{0.70}$ catalyst. The specific textural and chemical characteristics of prepared samples were identified by ICP-AES, XRD, XPS, NH_3-TPD, Py-IR, and nitrogen physisorption. Various parameters such as Ni/Cu molar ratio, reduction temperature, and reaction solvent played a great role in LA hydrogenation. The recycling experiments revealed that reactivated $Ni_{4.59}Cu_1Mg_{1.58}Al_{1.96}Fe_{0.70}$ maintained excellent activity, stability, and magnetism after being used five times, which made $Ni_{4.59}Cu_1Mg_{1.58}Al_{1.96}Fe_{0.70}$ a potential catalyst for the production of GVL in industry.

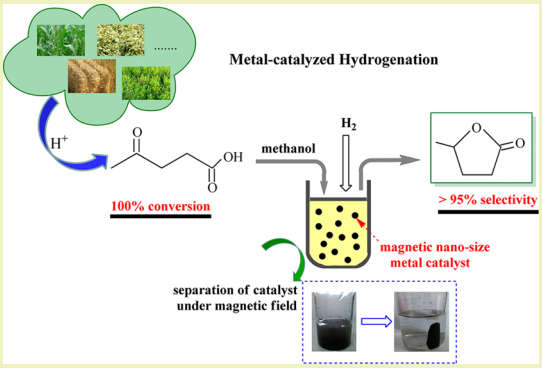

KEYWORDS: *Biomass, Hydrogenation, Levulinic acid, Magnetic catalyst, γ-Valerolactone*

INTRODUCTION

With gradual depletion of fossil resources and further deterioration of global climate, increasing concerns are paid to the production of fuels and chemicals from sustainable resources.[1,2] Biomass, which is widespread, renewable, low-cost, and abundant, is regarded as a promising alternative for fossil resources. Currently, extensive work has been directed toward converting biomass into various value-added chemicals.[3−6] Among these platform compounds, γ-valerolactone (GVL) is suited for use as a versatile building block for the production of valuable chemicals and high-grade fuels,[7−9] which has attracted worldwide attention.

Typically, targeted GVL production can be achieved through hydrogenation and subsequent cyclization of levulinic acid (LA), either using heterogeneous or homogeneous catalysts.[10−15] Published literatures indicated that homogeneous Ru-based catalysts presented superior activity toward the selective transformation of LA into GVL.[16−18] Desirable LA conversion and good GVL selectivity could be easily attained. However, the recycle and separation of these homogeneous catalysts after reaction were still a big problem. Therefore, heterogeneous catalysts are in great demand and have been advanced due to the advantages of high activity, easy separation, and recycling. In this case, noble metal catalysts, such as Ru/C, Ru/TiO_2, Pd/MCM-41, etc., displayed remarkable activity in LA hydrogenation.[19−22] Yan et al. reported that 96.5% yield of GVL was obtained using Pd/SiO_2 under the conditions of 453 K and 9.0 MPa H_2 in aqueous phase.[23] Manzer systematically investigated LA hydrogenation under 5.5 MPa H_2 over various catalysts and pointed out that Ru/C gave the highest GVL yield at 97% in dioxane solvent.[24] Although desirable results were achieved using supported noble metal catalysts, the obvious drawback of being high cost limited the practical application of these catalysts in large-scale GVL production. Besides, Ru nanocatalysts showed slow deactivation due to carbon deposition, acid-assisted metal loss, and structural changes of support.[19,22] Therefore, the development of cheap, highly active, stable, and readily recyclable catalysts remains an urgent problem in the present studies.

In recent years, inexpensive hydrotalcite-like compounds (HTlcs), composed of divalent and/or trivalent metals such as Ni, Cu, Co, Al, etc., exhibited great catalytic activity and stability in hydrogenation, polymerization, isomerization, and reforming reactions as well as oxidation reactions and so on because the catalysts derived from HTlcs generally had smaller crystal size, large surface area, high stability against sintering, good reducibility, and high dispersion of active phases.[25−29]

Received: March 18, 2015
Published: July 6, 2015

DOI: 10.1021/acssuschemeng.5b00535
ACS Sustainable Chem. Eng. 2015, 3, 1708−1714

Among these HTlc-derived catalysts, Ni- and Cu-based catalysts were widely applied in hydrogenation reactions.[30,31] In this respect, Yan et al. had synthesized Cu-catalysts derived from HTlcs for efficient hydrogenation of biomass-derived furfural and LA, whereby promising yields in target products (95% furfuryl alcohol and 91% GVL) were achieved at a temperature of 473 K.[32,33] Besides, compositions including Fe^{3+}, Cr^{3+}, and Al^{3+}, characteristic of high electronegativity, were found to favor the hydrogenation of the C═O bond.[34,35] It is important to note that magnetic Fe and Co elements markedly elevated the hydrogenation rate, as well as help the magnetic separation of catalysts from the mixtures.[36]

In this work, a series of low-cost and magnetic Ni/Cu/Al/Fe catalysts derived from hydrotalcite-like compounds were synthesized and introduced in LA hydrogenation. Various metal-modified catalysts were also developed to find the most active one for selective hydrogenation of LA into GVL. Effects of varied experiment parameters were systematically investigated, including reduction temperature, Ni/Cu molar ratio, initial pressure, reaction solvents, and so on. To our delight, 98.1% yield of GVL was obtained with a TOF value of 1.98 $m_{GVL}\ m_{(Ni+Cu)}^{-1}\ h^{-1}$ under the optimized conditions; moreover, the prepared magnetic catalyst showed excellent activity and stability in recycling experiments.

EXPERIMENTAL SECTION

Sections including Materials, Catalyst preparation, Characterizations, and Product analysis are described in detail in the Supporting Information.

Catalytic Reaction Procedure. In a typical reaction, the high pressure autoclave was loaded with magnetic catalyst, LA, and methanol purged four times with H_2 after which the reactor was pressurized with 2 MPa H_2 at room temperature. Then, the reaction was carried out at a certain temperature with a stirring rate of 500 rpm. After the reaction, the reactor was cooled to room temperature, followed by releasing residual H_2, and then liquid products were collected. The catalyst was separated by a magnet, rinsed with deionized water, and finally reactivated under H_2 atmosphere at 773 K before its next use.

RESULTS AND DISCUSSION

Catalyst Characterization. The synthesis of multi-element metallic HTlcs was carried out at Ni:Cu molar ratios from 0.93:1 to 9.21:1 by a co-precipitation method, and Table 1 lists the main components of prepared catalysts. The X-ray diffraction (XRD) patterns of Ni/Cu/Al/Fe hydrotalcite precursors (Figure 1a) exhibited several obvious diffraction peaks at 11.6°, 23.2°, 34.8°, 39.0°, 47.1°, and 61.8°, which were indexed to (003), (006), (012), (015), (018), and (113) reflections of hydrotalcite (JCPDS files no. 22-0700), respectively.[25,37] The sharp and symmetrical reflections were observed for (003), (006), (012), and (113) planes as well as broad and asymmetric reflections for (015) and (018) planes, indicating that the precursors were characteristic of a well-crystallized HT in carbonate form.[38] No isolated phases of individual metal hydroxides were detected, suggesting the formation of a pure hydrotalcite phase.

Table 1. Chemical Composition of HTlcs and Names of Obtained Catalysts

catalysts	catalyst precursors (denoted with the molar ratio of metals)	chemical analysis (wt %) Ni	Cu	Al	Fe
M1	$Ni_{0.93}Cu_1Al_{0.51}Fe_{0.21}$	19.38	22.38	4.89	4.20
M2	$Ni_{2.78}Cu_1Al_{1.08}Fe_{0.44}$	31.01	12.02	5.50	4.67
M3	$Ni_{4.63}Cu_1Al_{1.82}Fe_{0.79}$	34.62	8.06	6.25	5.62
M4	$Ni_{8.09}Cu_1Al_{3.09}Fe_{1.27}$	33.62	4.44	5.82	4.99
M5	$Ni_{9.21}Cu_1Al_{2.31}Fe_{0.47}$	58.20	6.32	6.21	2.64
M6	[a]$Ni_{4.65}Cu_1Co_{0.92}\ Al_{1.96}Fe_{0.74}$	27.60	6.39	5.32	4.15
M7	[b]$Ni_{4.65}Cu_1Zn_{1.20}Al_{2.58}Fe_{0.74}$	29.46	6.82	7.48	4.46
M8	[c]$Ni_{4.59}Cu_1Mg_{1.58}Al_{1.96}Fe_{0.70}$	31.79	7.45	6.20	4.50

[a]Co: 5.46 wt %. [b]Zn: 8.38 wt %. [c]Mg: 4.45 wt %.

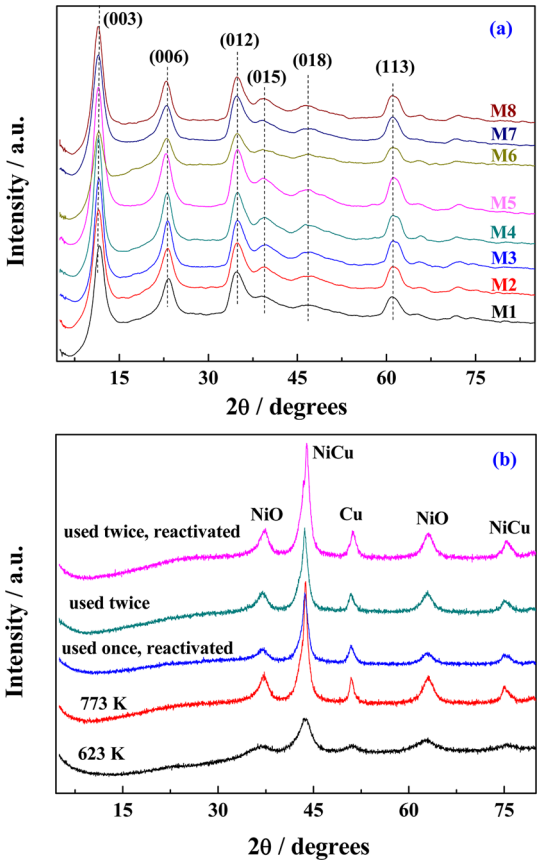

Figure 1. Powder XRD patterns of samples: (a) hydrotalcite precursors and (b) reduced M8 catalyst.

For reduced M8, several phases of metal species were clearly observed such as a NiCu alloy, NiO, and metallic Cu. As shown in Figure 1b, the presence of (111) and (220) phases at 2θ of 44.2° and 75.6° indicated the formation of a Ni−Cu solid solution, which could be assigned to a Ni-rich alloy.[39,40] The peak corresponding to planes (200) at 2θ of 51.7° demonstrated the presence of metallic Cu in face-center-cubic structure, which was in line with that given by JCPDS file no. 4-836. In terms of the NiO phase, characteristic peaks were found at 2θ of 37.3° (planes 110) and 63.1° (planes 220).[41] Besides, it is an obvious fact that no new phases were identified in the XRD diagram of reduced M8 after higher temperature treatment and/or repeating use.

The primary aim for conducting X-ray photoelectron spectroscopy (XPS) analysis was to obtain relevant information with respect to the chemical environment of reduced catalysts. High-resolution scans of Cu 2p and Ni 2p XPS spectra with different intensity scales as ordinate are shown in Figure 2A and

DOI: 10.1021/acssuschemeng.5b00535
ACS Sustainable Chem. Eng. 2015, 3, 1708−1714

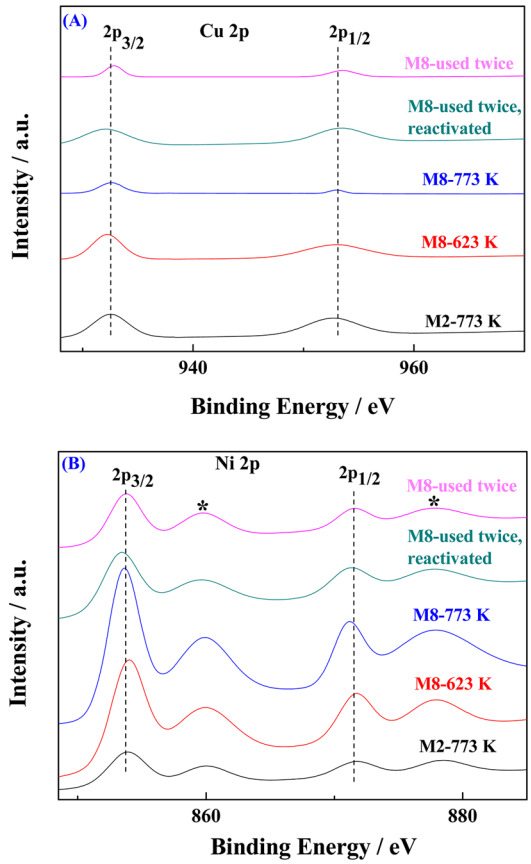

Figure 2. XPS spectra of reduced precursors: (A) Cu 2p and (B) Ni 2p.

B. For Cu 2p XPS, two obvious peaks at binding energies of 932.4 and 953.5 eV were detected, which could be definitely assigned to Cu $2p_{3/2}$ and $2p_{1/2}$, respectively. It is worth noting that the binding energies of metallic Cu are around 932.6 and 953.8 eV.[42,43] For this reason, the binding energies of Cu 2p in reduced samples were similar to that of Cu^0, confirming that the Cu element was essentially present in zero valence state after being activated at 623 K or higher temperatures.

In the case of Ni 2p XPS, the peaks of Ni $2p_{3/2}$ and $2p_{1/2}$ in reduced M2 and M8 catalysts were found at binding energies of around 853.8 and 871.4 eV, accompanying with two satellites at about 860.0 and 878.0 eV respectively. However, the binding energies of Ni $2p_{3/2}$ and $2p_{1/2}$ in zero-valence nickel were around 852.9 and 870.0 eV, respectively. The obtained binding energies of Ni $2p_{3/2}$, $2p_{1/2}$ and related satellites were among that of Ni^0 and Ni^{2+},[44,45] indicating the existence of metallic Ni and NiO species. The results were in accordance with those described in the XRD test. Through calculating the related areas in Ni 2p XPS of the M8 catalyst, active Ni^0 accounted for about 38.0% at the reduction temperature of 773 K, as compared to that of 24.3% at 623 K (Figure S1, Supporting Information). Besides, a negligible shift in the binding energies of recycled catalysts was determined, implying that the Ni and Cu sites maintained good activity even after repeated use.

The temperature-programmed desorption (TPD) profiles of desorbed ammonia on various catalysts were described in Figure 3, with related acidity present in the inset. The specific desorption temperature of NH_3-TPD reflects the acid strength of the catalyst, i.e., the higher temperature of desorption is, the stronger the acid strength is. It can be clearly seen that a higher

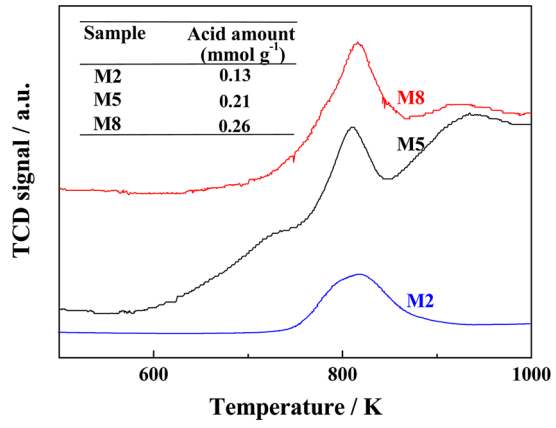

Figure 3. NH_3-TPD profiles of M2, M5, and M8 catalysts.

desorption temperature appears at around 816 and 935 K, with respect to M5 and M8 catalysts, respectively. However, the strong site at 935 K disappeared in the M2 catalyst, resulting in weaker acid strength (0.13 mmol g^{-1}). By contrast, M5 and M8 catalysts had higher acid amounts, owing to relatively larger amounts of the aluminum sites. With in-depth study, the IR spectra of adsorbed pyridine on the M5 catalyst were undertaken to characterize acid type and further confirm related concentration. As described in Figure S2 of the Supporting Information, bands at around 1441, 1488, and 1589 cm^{-1} attributed to pyridine molecules were apparently observed, suggesting the presence of Lewis acid sites in M5.[46−48] It is important to note that a characteristic band at 1540 cm^{-1} depicted as Brønsted acid was not found. In addition, the acid amount of M5 calculated according to Py-IR analysis was 0.22 mmol g^{-1}, which roughly agreed with the result from the NH_3-TPD profile.

The mesoporosity of recycled M8 was confirmed by N_2 adsorption−desorption isotherm analysis, as described in Figures S3 and S4 of the Supporting Information. All samples displayed type II isotherms with a type H2 hysteresis loop, characteristic of a mesoporous structure in a size range of 2−50 nm. Recycled samples displayed large adsorption volumes in the monolayer region, featuring a porous structure with uniformly particle size distribution. Table 2 summarizes the

Table 2. Properties of Recycled M8 Catalysts

sample	BET surface area (m^2 g^{-1})	average pore diameter (nm)	total pore volume (cm^3 g^{-1})
fresh	131.8	8.5	0.337
used once, RA	128.9	9.1	0.334
used twice	121.0	11.1	0.293
used twice, RA	120.1	11.2	0.281

RA: reactivated in H_2 atmosphere at 773 K.

related specific surface area using the BET method. The fresh M8 had a BET surface area of 131.8 m^2 g^{-1} and a total pore volume of 0.337 cm^3 g^{-1}. For regenerated catalysts, only a slight decrease in the BET surface area and total pore volume were achieved, verifying that reactivation treatment could be an effective way to defer rapid deactivation of the M8 catalyst. Meanwhile, high-temperature treatment helped particle sintering that resulted in a minor increase in pore diameter. As shown in Figure S5 of the Supporting Information, the phenomenon of particle agglomeration was apparently observed in recycling

DOI: 10.1021/acssuschemeng.5b00535
ACS Sustainable Chem. Eng. 2015, 3, 1708−1714

experiments, which might not provide good interactions between the substrate and active sites.

ACTIVITY TESTS

The activities of resultant M1 to M8 catalysts are evaluated in LA hydrogenation, and the results are depicted in Figure 4. It is

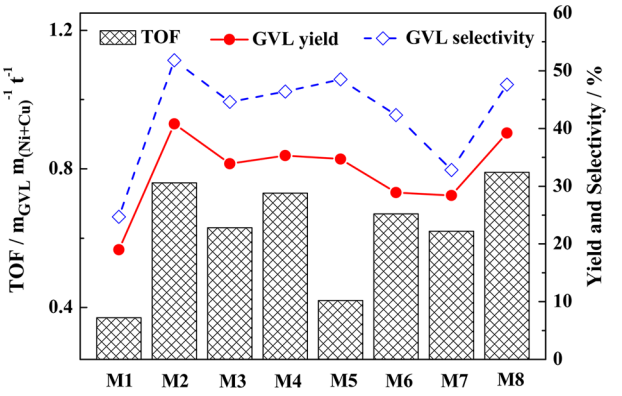

Figure 4. Effect of catalyst type on LA hydrogenation. Reaction conditions: LA (476 mg, 4.1 mmol), catalyst (119 mg, 25 wt % relative to LA), methanol (20 mL), H_2 (2.0 MPa), 395 K, and 3 h.

clearly evident that properly higher nickel content enhanced the reaction rate, and LA adsorbed on the active Ni/Cu sites was hydrogenated into GVL in quantity. However, a further increase in nickel component in M3−M5 led to a marked decline in related activity. Combined with the result of XPS analysis, Ni^{2+} species in the prepared precursors was hard to be totally reduced into Ni^0 even at a high temperature of 773 K. On the other hand, the practical content of active Cu^0 in M3−M5 was lowered relatively, thus rendering mild activity toward GVL formation. With the in-depth study, various metal elements such as Co-, Zn-, and Mg-modified catalysts were synthesized and applied in yielding GVL. In this respect, the M8 catalyst gave higher reaction rate at a TOF value of 0.79 m_{GVL} $m_{(Ni+Cu)}^{-1}$ t^{-1}, probably due to a synergistic effect among those metal elements. Under the catalyzing of M1 to M8 at a temperature of 395 K, much 4-hydroxyvaleric acid (HA) and methyl levulinate (ML) were observed during the reaction, resulting in a moderate selectivity to GVL.

Table 3 depicts the catalytic performance of randomly selected M2, M5, and M8 catalysts under various reaction temperatures. Generally, elevated temperature promoted LA conversion and GVL formation. A LA conversion of around 100% and GVL yield of 98.1% were achieved over the M8 catalyst, with increasing temperature up to 415 K. The same upward trends in GVL yield and TOF value were also observed on M2 and M5 samples since increased temperature accelerated the hydrogenation rate. However, significant decreases in GVL yield and selectivity at a higher temperature of 435 K were obtained for M2 and M8 catalysts, attributing to undesired side reactions such as deep hydrogenation and hydrogenolysis. It is worth mentioning that the GVL yield fell to 36.6% at 435 K over the M8 catalyst, as compared with that of 98.1% for 415 K. Interestingly, the M5 catalyst exhibited a relatively slower reaction rate in yielding GVL, if compared to M2 and M8.

On the basis of the above observations, a temperature of 415 K was chosen for the subsequent studies. The influence of catalyst loading on reaction rate and GVL selectivity was deeply investigated, as shown in Figure 5. One can clearly observe that

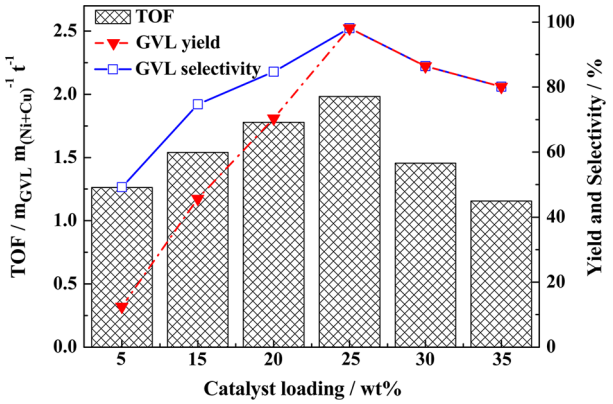

Figure 5. Effect of catalyst dosage on LA hydrogenation. Reaction conditions: LA (476 mg, 4.1 mmol), M8 catalyst, methanol (20 mL), H_2 (2.0 MPa), 3 h, and 415 K.

the TOF value and GVL selectivity were higher for a larger dosage during the 3 h of reaction. A significant rise in GVL yield, from 12.5 to 70.4%, was achieved when increasing dosage from 5 to 20 wt % relative to LA. This is because much more active sites were available during the reaction, thus resulting in a faster reaction rate to promote the conversion of LA to GVL. When setting loading at 25 wt %, a promising selectivity toward GVL was deserved at 98.1%, with a desirable TOF value of 1.98 m_{GVL} $m_{(Ni+Cu)}^{-1}$ h^{-1}. However, a further increase in catalyst loading led to a steep drop in GVL yield and selectivity, which could be elucidated as the occurrence of side effect (Figure S6, Supporting Information).

Figure 6 illustrates the effect of initial H_2 pressure ranging from 0 to 4.0 MPa on the hydrogenation of LA into GVL.

Table 3. Effect of Reaction Temperature on LA Hydrogenation

	M2			M5			M8		
temp. (K)	yield	selectivity	TOF	yield	selectivity	TOF	yield	selectivity	TOF
375	5.2	20.5	0.097	2.1	13.4	0.026	4.9	13.9	0.10
385	18.0	24.3	0.33	7.0	20.4	0.085	24.3	38.5	0.49
395	40.8	51.8	0.76	34.7	46.4	0.42	39.3	47.7	0.79
405	48.1	48.1	0.89	45.1	45.1	0.55	75.9	75.9	1.53
415	78.5	78.5	1.46	54.3	54.3	0.66	98.1	98.1	1.98
425	94.8	94.8	1.76	75.4	75.4	0.92	84.1	84.1	1.70
435	79.4	79.4	1.47	77.7	77.7	0.95	36.6	36.6	0.74

Reaction conditions: LA (476 mg, 4.1 mmol), catalyst (119 mg, 25 wt % relative to LA), methanol (20 mL), H_2 (2.0 MPa), and 3 h. Yield: GVL yield, %; selectivity: GVL selectivity, %; TOF: m_{GVL} $m_{(Ni+Cu)}^{-1}$ h^{-1}.

DOI: 10.1021/acssuschemeng.5b00535
ACS Sustainable Chem. Eng. 2015, 3, 1708−1714

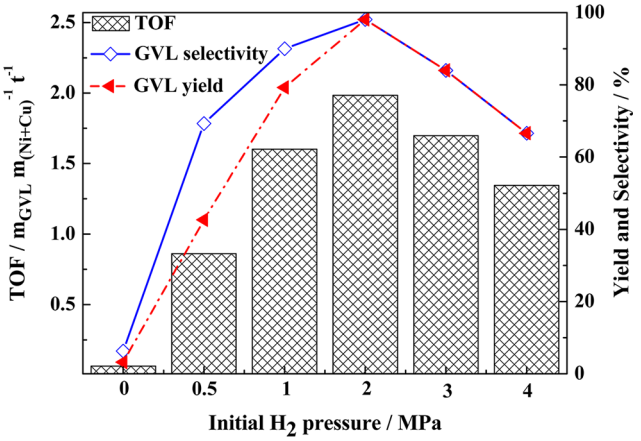

Figure 6. Effect of initial H_2 pressure on LA hydrogenation. Reaction conditions: LA (476 mg, 4.1 mmol), M8 catalyst (119 mg), methanol (20 mL), 415 K, and 3 h.

When no H_2 was filled, only a 3.2% GVL yield and the lowest reaction rate of 0.065 m_{GVL} $m_{(Ni+Cu)}^{-1}$ h^{-1} were attained. At this point, much ML was formed through the acid sites-promoted esterification of LA and methanol. Under H_2 atmosphere, targeted chemical GVL was generated in quantity, and the selectivity to GVL reached the maximum value at a pressure of 2.0 MPa. It is observed that higher hydrogen pressure enhanced the dissolved hydrogen concentration in methanol,[19] so much more hydrogen molecules could easily access Ni and Cu active sites, which accounted for the increased reaction rate at elevated pressure from 0.5 to 2.0 MPa. Nevertheless, a further increase in hydrogen pressure from 2.0 to 4.0 MPa led to an obvious drop in GVL selectivity, which could be illustrated as the appearance of deep hydrogenation of GVL to produce 2-methyltetrahydrofuran (Figure S7, Supporting Information). Taking into consideration practical cost and efficiency, the optimal initial hydrogen pressure for this reaction was suggested to be 2.0 MPa.

Given the outstanding performance of the M8 catalyst in yielding GVL, herein the influence of reduction temperature on catalyst activity was thoroughly surveyed. As shown in Figure 7, both TOF value and GVL yield increased significantly when raising the reduction temperature to 773 K. In this case, the highest GVL yield of 98.1% had been attained at a reaction rate

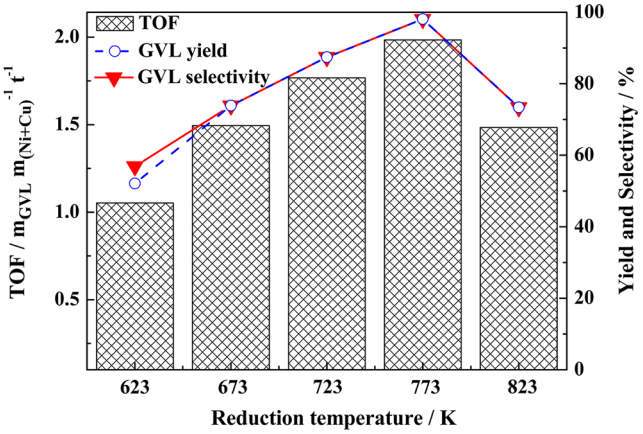

Figure 7. Effect of catalyst reduction temperature on LA hydrogenation. Reaction conditions: LA (476 mg, 4.1 mmol), M8 catalyst (119 mg), methanol (20 mL), H_2 (2.0 MPa), 415 K, and 3 h.

of 1.98 m_{GVL} $m_{(Ni+Cu)}^{-1}$ h^{-1}. The main reason is that much more active Ni^0 and Cu^0 were obtained through higher-temperature reduction (Figure S1, Supporting Information); therefore, the substrate LA would be hydrogenated into GVL in quantity. On the basis of the XPS analysis, full reduction of Cu^{2+} into metallic Cu in zero valence state could be achieved at around 623 K, while higher temperature was required to realize a complete reduction of Ni^{2+} to Ni^0, and this observation was in line with the previous work.[42] A further increased reduction temperature to 823 K, however, led to a remarkably reduced GVL selectivity to 73.4%, owing to the fact that the particle sintering occurred at high temperature (Figure S5, Supporting Information).

Table 4 presents the influence of reaction solvent on LA hydrogenation over M2, M5, and M8 catalysts. Interestingly,

Table 4. Effect of Reaction Solvent on LA Hydrogenation

catalysts	TOF (m_{GVL} $m_{(Ni+Cu)}^{-1}$ h^{-1})	GVL yield (%)	GVL selectivity (%)
M2 (water)	1.20	64.9	64.9
M2 (methanol)	1.46	78.5	78.5
M5 (water)	0.73	59.4	59.4
M5 (methanol)	0.68	55.4	55.4
M8 (water)	1.36	67.5	67.5
M8 (methanol)	1.98	98.1	98.1

Reaction conditions: LA (476 mg, 4.1 mmol), catalyst (119 mg), solvent (20 mL), H_2 (2.0 MPa), 415 K, and 3 h.

the LA was almost completely consumed in both water and methanol media. The higher activity was achieved on M2 and M8 catalysts in methanol, which displayed a higher GVL yield and TOF value. Furthermore, it is clear that the reaction rate and selectivity to GVL were relatively lower in the aqueous phase, in comparison with that of methanol. Much intermediate HA was first formed through the aqueous phase hydrogenation of carbonyl in LA, followed by further conversion into GVL. In regards to the M5 catalyst, comparable yield and selectivity in GVL were observed when reacted in methanol and water, endowing these two systems with similar TOF values of around 0.70 m_{GVL} $m_{(Ni+Cu)}^{-1}$ h^{-1}. All things considered, magnetic Ni/Cu/Al/Fe catalysts were more suitable for converting LA into GVL in the methanol system.

To further examine the stability, recycling experiments on the hydrogenation of LA into GVL were done with the M8 catalyst. As observed in Figure 8, a significant decline in reaction rate and GVL yield had been evidently displayed when the spent catalyst was used for the second time without being reactivated. In the following runs, the catalyst activity was maintained at moderate level with a TOF value of around 1.20 m_{GVL} $m_{(Ni+Cu)}^{-1}$ h^{-1}. As was confirmed by related characterizations, such as XPS, TEM, BET, and ICP-AES analyses, adsorbed carbohydrates, particle agglomeration, and Ni leaching (Table S1, Supporting Information) would lead to a lower level of activity in recycled catalysts to some extent. As a comparison, reactivation of recycled M8 under H_2 atmosphere was found to be an effective way to promote hydrogenation activity, where reactivated M8 sustained good catalytic activity after the consecutive cycles. This was mainly because many more active sites were available after the reactivation treatment. Comparing the catalytic activity of M8 with other noble metal catalysts (Table S2, Supporting Information), M8 presented the lowest TOF value for GVL production in term of reaction rate.

DOI: 10.1021/acssuschemeng.5b00535
ACS Sustainable Chem. Eng. 2015, 3, 1708−1714

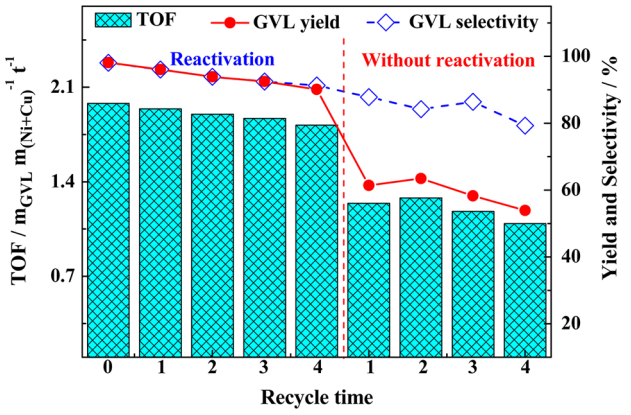

Figure 8. Effect of catalyst recycling on LA hydrogenation. Reaction conditions: LA (476 mg, 4.1 mmol), M8 catalyst (119 mg), methanol (20 mL), H_2 (2.0 MPa), 415 K, and 3 h.

Particularly, great yield and selectivity to GVL were attained on the M8 catalyst, which was comparable with that of Ru/C. However, it is notable that a significant decrease in the activity of recycled Ru/C was observed, in case that reactivation treatment was not performed. After a comprehensive comparison, magnetic M8, mainly composed of active Ni and Cu sites, still was a good candidate for catalytic conversion of LA into GVL.

CONCLUSIONS

We have developed a series of cheap and magnetic Ni/Cu/Al/Fe catalysts for the selective hydrogenation of LA into GVL. Among the prepared catalysts, $Ni_{4.59}Cu_1Mg_{1.58}Al_{1.96}Fe_{0.70}$ was found to be the most active, and the highest GVL yield of 98.1% had been achieved at 415 K under 2.0 MPa H_2 after a reaction of 3 h. Moreover, the recovery and reutilizations of catalyst in successive reactions suggest that the magnetic catalyst could be recycled for more than five cycles without being defeated in its performance, demonstrating that it is a promising candidate to produce valuable GVL through LA hydrogenation.

ASSOCIATED CONTENT

Supporting Information

Materials, catalyst preparation, characterizations, product analysis, and proposed reaction mechanism. The Supporting Information is available free of charge on the ACS Publications website at DOI: 10.1021/acssuschemeng.5b00535.

AUTHOR INFORMATION

Corresponding Author

*Tel./Fax: (+86)-20-3722-3380. E-mail: chenjz@ms.giec.ac.cn.

Notes

The authors declare no competing financial interest.

ACKNOWLEDGMENTS

This work was supported by Natural Science Foundation of Guangdong Province (2014A030310386), National Basic Research Program of China (973 Program, 2012CB215304), National Natural Science Foundation of China (21472189), and Open Fund of Key Laboratory of Renewable Energy, Chinese Academy of Sciences (y507ja1001).

REFERENCES

(1) Kunkes, E. L.; Simonetti, D. A.; West, R. M.; Serrano-Ruiz, J. C.; Gärtner, C. A.; Dumesic, J. A. Catalytic conversion of biomass to monofunctional hydrocarbons and targeted liquid-fuel classes. *Science* **2008**, *322*, 417−421.

(2) Huber, G. W.; Iborra, S.; Corma, A. Synthesis of transportation fuels from biomass: chemistry, catalysts, and engineering. *Chem. Rev.* **2006**, *106*, 4044−4098.

(3) Selva, M.; Gottardo, M.; Perosa, A. Upgrade of biomass-derived levulinic acid via Ru/C-catalyzed hydrogenation to γ-valerolactone in aqueous-organic-ionic liquids multiphase systems. *ACS Sustainable Chem. Eng.* **2013**, *1*, 180−189.

(4) Zhang, J.; Wu, S. B.; Li, B.; Zhang, H. D. Advances in the catalytic production of valuable levulinic acid derivatives. *ChemCatChem* **2012**, *4*, 1230−1237.

(5) Zhang, W.; Chen, J. Z.; Liu, R. L.; Wang, S. P.; Chen, L. M.; Li, K. G. Hydrodeoxygenation of lignin-derived phenolic monomers and dimers to alkane fuels over bifunctional zeolite-supported metal catalysts. *ACS Sustainable Chem. Eng.* **2014**, *2*, 683−691.

(6) Zhang, J.; Li, J. B.; Wu, S. B.; Liu, Y. Advances in the catalytic production and utilization of sorbitol. *Ind. Eng. Chem. Res.* **2013**, *52*, 11799−11815.

(7) Horváth, I. T.; Mehdi, H.; Fábos, V.; Boda, L.; Mika, L. T. γ-Valerolactone—a sustainable liquid for energy and carbon-based chemicals. *Green Chem.* **2008**, *10*, 238−242.

(8) Mascal, M.; Dutta, S.; Gandarias, I. Hydrodeoxygenation of the angelica lactone dimer, a cellulose-based feedstock: simple, high-yield synthesis of branched C_7−C_{10} gasoline-like hydrocarbons. *Angew. Chem., Int. Ed.* **2014**, *53*, 1854−1857.

(9) Corma, A.; de la Torre, O.; Renz, M.; Villandier, N. Production of high-quality diesel from biomass waste products. *Angew. Chem., Int. Ed.* **2011**, *50*, 2375−2378.

(10) Mai, E. F.; Machado, M. A.; Davies, T. E.; Lopez-Sanchez, J. A.; Teixeira da Silva, V. Molybdenum carbide nanoparticles within carbonnanotubes as superior catalysts for γ-valerolactone production via levulinic acid hydrogenation. *Green Chem.* **2014**, *16*, 4092−4097.

(11) Galleti, A. M. R.; Antonetti, G.; De Luise, V.; Martinelli, M. A sustainable process for the production of γ-valerolactone by hydrogenation of biomass-derived levulinic acid. *Green Chem.* **2012**, *14*, 688−694.

(12) Chia, M.; Dumesic, J. A. Liquid-phase catalytic transfer hydrogenation and cyclization of levulinic acid and its esters to γ-valerolactone over metal oxide catalysts. *Chem. Commun.* **2011**, *47*, 12233−12235.

(13) Wright, W. R. H.; Palkovits, R. Development of heterogeneous catalysts for the conversion of levulinic acid to γ-valerolactone. *ChemSusChem* **2012**, *5*, 1657−1667.

(14) Deng, L.; Li, J.; Lai, D.-M.; Fu, Y.; Guo, Q.-X. Catalytic conversion of biomass-derived carbohydrates into γ-valerolactone without using an external H_2 supply. *Angew. Chem., Int. Ed.* **2009**, *48*, 6529−6532.

(15) Du, X. L.; He, L.; Zhao, S.; Liu, Y.-M.; Cao, Y.; He, H.-Y.; Fan, K. N. Hydrogen-independent reductive transformation of carbohydrate biomass into γ-valerolactone and pyrrolidone derivatives with supported gold catalysts. *Angew. Chem., Int. Ed.* **2011**, *50*, 7815−7819.

(16) Geilen, F. M. A.; Engendahl, B.; Harwardt, A.; Marquardt, W.; Klankermayer, J.; Leitner, W. Selective and flexible transformation of biomass-derived platform chemicals by a multifunctional catalytic system. *Angew. Chem., Int. Ed.* **2010**, *49*, 5510−5514.

(17) Geilen, F. M. A.; Engendahl, B.; Hölscher, M.; Klankermayer, J.; Leitner, W. Selective homogeneous hydrogenation of biogenic carboxylic acids with $[Ru(TriPhos)H]^+$: a mechanistic study. *J. Am. Chem. Soc.* **2011**, *133*, 14349−14358.

(18) Mehdi, H.; Fábos, V.; Tuba, R.; Bodor, A.; Mika, L. T.; Horváth, I. T. Integration of homogeneous and heterogeneous catalytic processes for a multi-step conversion of biomass: from sucrose to levulinic acid, γ-valerolactone, 1,4-pentanediol, 2-methyl-tetrahydrofuran, and alkanes. *Top. Catal.* **2008**, *48*, 49−54.

DOI: 10.1021/acssuschemeng.5b00535
ACS Sustainable Chem. Eng. 2015, 3, 1708−1714

(19) Yan, Z. P.; Lin, L.; Liu, S. J. Synthesis of γ-valerolactone by hydrogenation of biomass-derived levulinic acid over Ru/C catalyst. *Energy Fuels* **2009**, *23*, 3853−3858.
(20) Yan, K.; Lafleur, T.; Jarvis, C.; Wu, G. S. Clean and selective production of γ-valerolactone from biomass-derived levulinic acid catalyzed by recyclable Pd nanoparticle catalyst. *J. Cleaner Prod.* **2014**, *72*, 230−232.
(21) Sudhakar, M.; Lakshmi Kantam, M.; Swarna Jaya, V. S.; Kishore, R.; Ramanujachary, K. V.; Venugopal, A. Hydroxyapatite as a novel support for Ru in the hydrogenation of levulinic acid to γ-valerolactone. *Catal. Commun.* **2014**, *50*, 101−104.
(22) Luo, W. H.; Deka, U.; Beale, A. M.; van Eck, E. R. H.; Bruijnincx, P. C. A.; Weckhuysen, B. M. Ruthenium-catalyzed hydrogenation of levulinic acid: Influence of the support and solvent on catalyst selectivity and stability. *J. Catal.* **2013**, *301*, 175−186.
(23) Yan, K.; Lafleur, T.; Wu, G.; Liao, J.; Ceng, C.; Xie, X. Highly selective production of value-added γ-valerolactone from biomass-derived levulinic acid using the robust Pd nanoparticles. *Appl. Catal., A* **2013**, *468*, 52−58.
(24) Manzer, L. E. Catalytic synthesis of α-methylene-γ-valerolactone: a biomass-derived acrylic monomer. *Appl. Catal., A* **2004**, *272*, 249−256.
(25) Cavani, F.; Trifiro, F.; Vaccari, A. Hydrotalcite-type anionic clays: preparation, properties and applications. *Catal. Today* **1991**, *11*, 173−301.
(26) Galvita, V.; Siddiqi, G.; Sun, P. P.; Bell, A. T. Ethane dehydrogenation on Pt/Mg(Al)O and PtSn/Mg(Al)O catalysts. *J. Catal.* **2010**, *271*, 209−219.
(27) Sharma, S. K.; Parikh, P. A.; Jasra, R. V. Eco-friendly synthesis of jasminaldehyde by condensation of 1-heptanal with benzaldehyde using hydrotalcite as a solid base catalyst. *J. Mol. Catal. A: Chem.* **2008**, *286*, 55−62.
(28) Basile, F.; Benito, P.; Fornasari, G.; Gazzoli, D.; Pettiti, I.; Rosetti, V.; Vaccari, A. Ni-catalysts obtained from silicate intercalated HTlcs active in the catalytic partial oxidation of methane: Influence of the silicate content. *Catal. Today* **2009**, *142*, 78−84.
(29) Cruz, I. O.; Ribeiro, N. F. P.; Aranda, D. A. G.; Souza, M. M. V. M Hydrogen production by aqueous-phase reforming of ethanol over nickel catalysts prepared from hydrotalcite precursors. *Catal. Commun.* **2008**, *9*, 2606−2611.
(30) Upare, P. P.; Lee, J. M.; Hwang, Y. K.; Hwang, D. W.; Lee, J. H.; Halligudi, S. B.; Hwang, J. S.; Chang, J. S. Direct hydrocyclization of biomass-derived levulinic acid to 2-methyltetrahydrofuran over nanocomposite copper/silica catalysts. *ChemSusChem* **2011**, *4*, 1749−1752.
(31) Shimizu, K.; Kanno, S.; Kon, K. Hydrogenation of levulinic acid to γ-valerolactone by Ni and MoO_x co-loaded carbon catalysts. *Green Chem.* **2014**, *16*, 3899−3903.
(32) Yan, K.; Liao, J. Y.; Wu, X.; Xie, X. M. A noble-metal free Cu-catalyst derived from hydrotalcite for highly efficient hydrogenation of biomass-derived furfural and levulinic acid. *RSC Adv.* **2013**, *3*, 3853−3856.
(33) Yan, K.; Chen, A. C. Efficient hydrogenation of biomass-derived furfural and levulinic acid on the facilely synthesized noble-metal-free Cu-Cr catalyst. *Energy* **2013**, *58*, 357−363.
(34) Sitthisa, S.; Sooknoi, T.; Ma, Y. G.; Balbuena, P. B.; Resasco, D. E. Kinetics and mechanism of hydrogenation of furfural on Cu/SiO_2 catalysts. *J. Catal.* **2011**, *277*, 1−13.
(35) Zheng, H. Y.; Zhu, Y. L.; Teng, B. T.; Bai, Z. Q.; Zhang, C. H.; Xiang, H. W.; Li, Y. W. Towards understanding the reaction pathway in vapour phase hydrogenation of furfural to 2-methylfuran. *J. Mol. Catal. A: Chem.* **2006**, *246*, 18−23.
(36) Hoffer, B. W.; Crezee, E.; Mooijman, P. R. M.; van Langeveld, A. D.; Kapteijn, F.; Moulijn, J. A. Carbon supported Ru catalysts as promising alternative for Raney-type Ni in the selective hydrogenation of D-glucose. *Catal. Today* **2003**, *79−80*, 35−41.
(37) Kannan, S.; Rives, V.; Knözinger, H. High-temperature transformations of Cu-rich hydrotalcites. *J. Solid State Chem.* **2004**, *177*, 319−331.
(38) Courty, P.; Durand, D.; Freund, E.; Sugier, A. C_1-C_6 alcohols from synthesis gas on copper-cobalt catalysts. *J. Mol. Catal.* **1982**, *17*, 241−254.
(39) Wu, S. P.; Ni, P.; Jiao, L.; Zeng, Z. N. Preparation of ultra-fine copper−nickel bimetallic powders with hydrothermal-reduction method. *Mater. Chem. Phys.* **2007**, *105*, 71−75.
(40) Wu, S. P. Preparation of ultra fine nickel-copper bimetallic powder for BME-MLCC. *Microelectron. J.* **2007**, *38*, 41−46.
(41) Yi, H. H.; Zhao, S. Z.; Tang, X. L.; Ning, P.; Wang, H. Y.; He, D. Influence of calcination temperature on the hydrolysis of carbonyl sulfide over hydrotalcite-derived Zn−Ni−Al catalyst. *Catal. Commun.* **2011**, *12*, 1492−1495.
(42) Velu, S.; Suzuki, K.; Vijayaraj, M.; Barman, S.; Gopinath, C. S. In situ XPS investigations of $Cu_{1-x}Ni_xZnAl$-mixed metal oxide catalysts used in the oxidative steam reforming of bio-ethanol. *Appl. Catal., B* **2005**, *55*, 287−299.
(43) Strohmeier, B. R.; Leyden, D. E.; Field, R. S.; Hercules, D. M. Surface spectroscopic characterization of Cu/Al_2O_3. *J. Catal.* **1985**, *94*, 514−530.
(44) Hou, Z. Y.; Yokota, O.; Tanaka, T.; Yashima, T. Characterization of Ca-promoted Ni/α-Al_2O_3 catalyst for CH_4 reforming with CO_2. *Appl. Catal., A* **2003**, *253*, 381−387.
(45) Lenglet, M.; Hochu, F.; Durr, J.; Tuilier, M. H. Investigation of the chemical bonding in $3d^8$ nickel (II) charge transfer insulator (NiO, oxidic spinels) from ligand-field spectroscopy, Ni 2p XPS and X-ray absorption spectroscopy. *Solid State Commun.* **1997**, *104*, 793−798.
(46) Kondo, J. N.; Nishitani, R.; Yoda, E.; Yokoi, T.; Tatsumi, T.; Domen, K. A comparative IR characterization of acidic sites on HY zeolite by pyridine and CO probes with silica−alumina and γ-alumina references. *Phys. Chem. Chem. Phys.* **2010**, *12*, 11576−11586.
(47) Matsunaga, Y.; Yamazaki, H.; Yokoi, T.; Tatsumi, T.; Kondo, J. N. IR characterization of homogeneously mixed silica−alumina samples and dealuminated Y zeolites by using pyridine, CO, and propene probe molecules. *J. Phys. Chem. C* **2013**, *117*, 14043−14050.
(48) Emeis, C. A. Determination of integrated molar extinction coefficients for infrared absorption bands of pyridine adsorbed on solid acid catalysts. *J. Catal.* **1993**, *141*, 347−354.

DOI: 10.1021/acssuschemeng.5b00535
ACS Sustainable Chem. Eng. 2015, 3, 1708−1714